International Journal of Mathematical Archive-3(8), 2012, 3004-3015
Available online through www.ijma.info ISSN 2229 – 5046

FLOW AND HEAT TRANSFER AT A NONLINEARLY SHRINKING POROUS SHEET IN A THERMALLY STRATIFIED MEDIUM

K. V. Prasad*

Department of Mathematics, Bangalore University, Bangalore 560001, India

(Received on: 30-07-12; Revised & Accepted on: 22-08-12)

ABSTRACT

An analysis is carried out to study the laminar, boundary layer flow and heat transfer of a viscous fluid over shrinking permeable sheet with a power-law velocity in a thermally stratified environment. The sheet is assumed to shrink in its own plane with power-law velocity proportional to the distance from the stagnation point. The governing partial differential equations are first transformed into coupled non-linear ordinary differential equation using a similarity transformation. From here, we are able to compute several classes of exact solutions for certain values of the physical parameters. For other values of the physical parameters, the coupled non-linear boundary value problem is solved numerically by a second order finite difference scheme known as Keller Box method. Numerical computations are performed for two different cases namely, impermeable ($f_w = 0$) and permeable ($f_w \neq 0$) cases to get the effects of the thermally stratified environment on the velocity and temperature fields, at several physical situations. Numerical results for the skin-friction coefficient and the Nusselt number are tabulated for different values of the pertinent parameters. This is the first time such results for power-law nonlinearly shrinking sheets have been discussed in the context of a thermally stratified medium.

Keywords: *Stratified medium, shrinking sheet, finite differences, Keller-Box method, boundary layers, similarity solutions, heat transfer.*

1. INTRODUCTION

The study of two-dimensional boundary layer flow and heat transfer over a continuous moving surface with a given temperature, moving in an otherwise quiescent fluid, has attracted considerable attention during the past two decades due to their extensive applications to several industrial manufacturing processes. A few examples of such technological processes are the extrusion of plastic sheet, hot rolling, wire drawing, glass fiber, and paper production, drawing of plastic films, spinning and cooling of a metallic plate in a cooling bath [1-3]. This type of flow was first initiated by Sakiadis [4-5] over a continuously moving surface with constant speed. Numerous studies have been conducted thereafter to explore the flow characteristics for various applications. The thermal behavior of the problem was studied by Erickson et al. [6] and experimentally verified by Tsou et al. [7]. Crane [8] extended the work of Sakiadis [4] to the flow caused by an elastic sheet moving in its own plane with a velocity varying linearly with the distance from a fixed point. Following the work of Crane [8], the boundary conditions on the surface were generalized by other researchers [9-16]. A new solution branch of both impermeable and permeable stretching sheet was found recently by Liao [17-18]: This indicates that multiple solutions for the stretching surface problems are possible under certain conditions.

The physical situation discussed by Crane [8] is one of the possible cases. Another physical phenomenon is the flow of an incompressible viscous fluid over a shrinking sheet. Such situation occurs in the flow over a rising shrinking balloon. From the consideration of continuity, Crane's stretching sheet solution induces a far field suction toward the sheet, while flow over a shrinking sheet would give rise to a velocity away from the sheet. From a physical point of view, vorticity generated at the shrinking sheet is not confined within a boundary layer and a steady flow is not possible unless adequate suction is applied at the surface. A recent paper published by Miklavcic and Wang [19] investigates two-dimensional and axisymmetric viscous flows induced by a shrinking sheet in the presence of uniform surface suction. Fang [20] analyzed the boundary layer flow of a continuously shrinking sheet with a power-law surface velocity. The unsteady viscous flow over a continuously shrinking surface with mass suction was investigated by Fang et al. [21] and showed that the multiple solutions exist for a certain range of mass suction and the unsteady parameters. The shrinking sheet problem was extended to other types of fluids by Hayat et al. [22] and Sajid et al. [23]. For the flow induced by a shrinking sheet, it is essentially a backward flow (discussed by Glodstein [24]); for a backward flow

*Corresponding author: K. V. Prasad**
Department of Mathematics, Bangalore University, Bangalore 560001, India

configuration the fluid loses any memory of the perturbation induced by the leading ledge, say the slot. This flow has quite distinct physical phenomena from the forward stretching flow. Available literature on the flow over a shrinking sheet reveals that not much work is being carried out for viscous flow and heat transfer over a non-linear shrinking sheet in a thermally stratified environment.

Motivated by these various applications, in the present paper, we analyze the effects of thermally stratified environment on the viscous flow and heat transfer at a permeable non-linear shrinking sheet. This is a generalization of Henkes and Hoogendoorn [25], to the study the viscous fluid flow and heat transfer with a power-law (nonlinear) shrinking sheet. Here the momentum and energy equations are coupled nonlinear partial differential equations. These coupled nonlinear partial differential equations are reduced to coupled nonlinear ordinary differential equations by a similarity transformation and are solved numerically by an implicit finite difference method known as Keller box method.

2. MATHEMATICAL FORMULATION

Consider a laminar steady two-dimensional viscous flow over a continuously shrinking sheet in a quiescent fluid. The sheet shrinks in its own plane with a velocity proportional to the power of distance from the origin. The sheet shrinking-velocity is assumed to be $-u_w(x)$ where $u_w(x)$ is a positive function for all values of *x* and the mass transfer velocity at the wall is $\mathrm{v}_w = \mathrm{v}_w(x)$. The *x*-axis runs along the shrinking surface in the direction opposite to the sheet motion and *y*-axis is perpendicular to it. Assuming that the fluid is incompressible, the governing equations for the flow and heat transfer (in the absence of viscous dissipation) become:

$$\frac{\partial u}{\partial x} + \frac{\partial \mathrm{v}}{\partial y} = 0, \tag{1}$$

$$u\frac{\partial u}{\partial x} + \mathrm{v}\frac{\partial u}{\partial y} = -\frac{1}{\rho}\frac{\partial p}{\partial x} + \nu\left(\frac{\partial^2 u}{\partial x^2} + \frac{\partial^2 u}{\partial y^2}\right), \tag{2}$$

$$u\frac{\partial \mathrm{v}}{\partial x} + \mathrm{v}\frac{\partial \mathrm{v}}{\partial y} = -\frac{1}{\rho}\frac{\partial p}{\partial y} + \nu\left(\frac{\partial^2 \mathrm{v}}{\partial x^2} + \frac{\partial^2 \mathrm{v}}{\partial y^2}\right), \tag{3}$$

$$u\frac{\partial T}{\partial x} + \mathrm{v}\frac{\partial T}{\partial y} = \alpha\left(\frac{\partial^2 T}{\partial x^2} + \frac{\partial^2 T}{\partial y^2}\right), \tag{4}$$

where u and v are the velocity components in the x and y directions, respectively. *T* is the temperature, ρ the fluid density, *p* the fluid pressure, ν the kinematic viscosity, and α is the thermal diffusivity of the fluid. Based on the boundary layer approximation the term $\alpha\frac{\partial^2 T}{\partial x^2}$ has been neglected. For this boundary layer assumption, the solution is only valid at a sufficiently large distance from the leading point or shrinking slot. In addition, since we neglected the dissipation term in the energy equation, the current analysis is applicable to low Eckert number flows.

The appropriate boundary conditions for the problem are;

$$u = -u_w(x), \quad \mathrm{v} = \mathrm{v}_w(x), \quad T = T_w(x) \quad at \;\; y = 0, \tag{5a}$$

$$u = 0 \qquad T = T_\infty(x) \qquad as \;\; y \to \infty. \tag{5b}$$

In the equation (5) the negative sign indicates the shrinking sheet and $\mathrm{v}_w(x)$ is the mass flux velocity, with $\mathrm{v}_w(x) < 0$ for suction and $\mathrm{v}_w(x) > 0$ for blowing or injection respectively. The subscript *w* denotes the conditions at the wall. Here, $u_w(x)$, $T_w(x)$ and $T_\infty(x)$ are functions of *x* (and are assumed to vary in powers of *x*, the distance from the slot) and are defined as follows (for details see Henkes and Hoogendoorn [25] and Kulkarni et al. [26]):

$$u_w(x) = U_w(Mx+N)^m, \;\; T_w(x) = (n+1)\Delta T(Mx+N)^m + T_c,$$
$$T_\infty(x) = n\Delta T(Mx+N)^m + T_c, \tag{6}$$

where T_c is a constant, m is a power law exponent parameter for the shrinking sheet and is positive or negative (indicating respectively that the shrinking surface is accelerating or decelerating from the extruded slit), n is the wall temperature parameter describing the environment temperature for $n=0$ and fixed wall temperature for $n=-1$, *M* and *N* are (positive and non-negative, respectively) constants.

3. SIMILARITY TRANSFORMATION

Here, we are searching for solutions for the system (2)-(4) that describes the boundary layer flow over a shrinking sheet in a stratified environment [see the boundary conditions (5)]. Under a special situation a similarity solutions exist for equations (4). Such a similarity solution depends only on one coordinate η instead of the two independent variables x and y. Recently Semenov [27] has derived the conditions for all possible similarity solutions. The temperature field can be rewritten as,

$$T=\left(n+\theta(\eta)\right)\Delta T\,\xi^{m}+T_c, \tag{7}$$

and the transformed coordinates in the above expression are,

$$\xi=Mx+N,\quad \xi\geq 0 \text{ and } \eta=\left(\frac{U_w M}{\nu}\right)^{\frac{1}{2}}\xi^{\frac{m-1}{2}}\,y. \tag{8}$$

A stream function is introduced as

$$\psi=\left(\frac{\nu\,U_w}{M}\right)^{\frac{1}{2}}\xi\;f(\eta), \tag{9}$$

which defines the velocity components u and v as

$$u=U_w\xi^{m}\;f'(\eta),\qquad \mathrm{v}=-\frac{1}{2}\left(\frac{\nu\,U_w}{M}\right)^{\frac{1}{2}}\xi^{\frac{m-1}{2}}\,M\left\{(m+1)f(\eta)+(m-1)f'(\eta)\right\}, \tag{10}$$

so that we can write

$$\mathrm{v}_w(x)=-\frac{m+1}{2}\left(\frac{\nu\,U_w}{M}\right)^{\frac{1}{2}}\xi^{\frac{m-1}{2}}\,M\,f_w,$$

where f_w is a constant [for suction $(f_w>0)$ and injection $(f_w<0)$]. The velocity components $(u,\mathrm{v})=\left(\frac{\partial\psi}{\partial y},-\frac{\partial\psi}{\partial x}\right)$ given by equation (10) automatically satisfied the continuity equation (1). Substitution of these transformation expressions into equations (2) - (4), and the use of the usual boundary layer approximation, yields the following coupled, nonlinear ordinary differential equations for f and θ,

$$f'''+\frac{m+1}{2}f\;f''-m\,f'^{2}=0, \tag{11}$$

$$\theta''+\mathrm{Pr}\left(\frac{m+1}{2}f\;\theta'-m(n+\theta)f'\right)=0, \tag{12}$$

subject to the boundary conditions,

$$\eta=0:\;f(\eta)=f_w,\quad f'(\eta)=-1,\quad \theta(\eta)=1, \tag{13a}$$

$$\eta\to\infty:\;f'(\eta)=0,\;\theta(\eta)=0, \tag{13b}$$

where f_w is the lateral mass transfer parameter showing the strength of the mass at the shrinking sheet. Here, we have the following special situations, $n=0$ for the non-stratified environment and $n=-1$ for the fixed wall temperature

distribution. The environment is stably stratified for $\frac{dT_\infty}{dx} > 0$ or $m\ M\ n > 0$. Hence, if m and n are of the same sign the environment is stably stratified. The physical quantities of interest are the skin friction coefficient C_f and the Nusselt number Nu_ξ, which are defined by

$$C_f = \frac{\tau_w}{\rho u_w^2}, \quad Nu_\xi = \frac{\xi\ q_w}{k\left(T_w - T_\infty\right)}, \tag{14a}$$

where τ_w is the skin friction or shear stress along the surface and q_w is the heat flux from the surface of the shrinking sheet, which are given by,

$$\tau_w = -\mu\left(\frac{\partial u}{\partial y}\right)_{at\ y=0}, \ q_w = -k\left(\frac{\partial T}{\partial y}\right)_{at\ y=0}. \tag{14b}$$

Using (7)-(10), we obtain

$$\left(\frac{\mathrm{Re}_\xi}{M}\right)^{\frac{1}{2}} C_f = f''(0), \quad \left(\mathrm{Re}_\xi\, M\right)^{\frac{-1}{2}}\ Nu_\xi = -\theta'(0), \tag{14c}$$

where $\mathrm{Re}_\xi = \frac{U_w \xi^{m+1}}{\nu}$ is the local Reynolds number.

4. EXACT SOLUTIONS FOR SOME SPECIAL CASES

Here, we present exact solutions in certain special cases. Such solutions are useful and serve as a baseline for comparison with the solutions obtained via numerical schemes. Regarding the existence and uniqueness of solutions to the ordinary differential equation (11) subject to the boundary conditions (13), see Van Gorder et al. [28]. Regarding the existence of solutions to (12) subject to (13), see [29]. In such a problem, $\theta(\eta)$ is governed by a linear equation one the function $f(\eta)$ is known, which makes the existence and uniqueness results easier to obtain. Hence, once a solution for $f(\eta)$ is know, one can find the solution for $\theta(\eta)$ analytically or numerically.

4.1. Exponential solutions for the linearly shrinking sheet case

In the case of a linearly shrinking sheet (i.e., *m* = 1), we have an exact solution to (11) - (13) for $f(\eta)$ of the form

$$f(\eta) = C + \frac{1}{C} e^{-C\eta}. \tag{15}$$

In the case that $f_w = 2$, this reduces to $f(\eta) = 1 + e^{-\eta}$ (see, e.g., Miklavcic and Wang [19]). Meanwhile, we have the solution

$$f_+(\eta) = f_w - \frac{2}{f_w + \sqrt{f_w^{\,2} - 4}}\left(1 - \exp\left\{-\eta\left(\frac{f_w + \sqrt{f_w^{\,2} - 4}}{2}\right)\right\}\right), \tag{16}$$

Valid for all $f_w > 2$. (See, e.g., Van Gorder et al. [28] for these exact solutions, and Van Gorder [30] for a general method of obtaining such solutions.) The shear stress at the wall is then given by

$$f_+''(0) = \frac{f_w + \sqrt{f_w^{\,2} - 4}}{2} > 0. \tag{17}$$

Furthermore, we have a second solution of the form

$$f_-(\eta) = f_w - \frac{2}{f_w - \sqrt{f_w^{\,2} - 4}}\left(1 - \exp\left\{-\eta\left(\frac{f_w - \sqrt{f_w^{\,2} - 4}}{2}\right)\right\}\right), \tag{18}$$

which is physically meaningful and valid for all $f_w > 2$. For this second solution, the shear stress at the wall is given by

$$f''(0) = \frac{f_w - \sqrt{f_w^{\,2} - 4}}{2\sqrt{}} > 0. \tag{19}$$

Note that when $f_w < 2$ we have no solutions of the form (15) (see, for instance, Van Gorder and Vajravelu [31]).

4.2. Algebraic solutions for the shrinking sheet

Assuming a solution of the form

$$f(\eta) = \frac{A}{B + C\eta}, \tag{20}$$

we find that a solution to (11) subject to (13) may be given in this form only when $f_w = \sqrt{6}$, and that such a solution reads

$$f(\eta) = \frac{6}{\sqrt{6} + \eta}. \tag{21}$$

Note that such a solution exists for every value of *m*. That is to say, for every value of *m*, $f_w = \sqrt{6}$ implies that (21) is the exact solution to (11).

4.3. Solution for *m* = -1 in terms of Weierstrass's elliptic functions

In the case of *m* = -1, note that (11) becomes

$$f''' + f'^2 = 0. \tag{22}$$

Making the substitution $g = f'$ we have that

$$g'' + g^2 = 0, \tag{23}$$

subject to boundary conditions $g(0) = -1$ and $g(\infty) = 0$. The solution to this boundary value problem is found to be

$$g(\eta) = -2^{1/3}\wp\left(\frac{2^{1/6}}{6^{1/2}}\eta + \kappa, 0, 0\right), \tag{24}$$

where $\wp$ denotes Weierstrass's elliptic function, and the constant κ is defined by the implicit relation $2^{1/3}\wp(\kappa, 0, 0) = 1$. The value $\kappa \approx 1.122462048$ gives physically meaningful solutions. Integrating (24) once, we obtain the exact solution for (11):

$$f(\eta) = f_w - 2^{1/3}\int_0^\eta \wp\left(\frac{2^{1/6}}{6^{1/2}}\chi + \kappa, 0, 0\right) d\chi. \tag{25}$$

5. NUMERICAL METHOD

The equations (11) and (12) are highly non-linear, coupled ordinary differential equations of third-order and second-order, respectively. Exact analytical solutions are not possible for the complete set of equations (11) and (12) and therefore we have use an efficient numerical method with second order finite difference scheme known as Keller-Box method. The coupled boundary value problem (11) and (12) of third order in *f* and second order in θ, respectively, has been reduced to a system of five simultaneous ordinary differential equations of first order for five unknowns following the method of superposition (Na [32]). To solve the system of first order equations we require five initial conditions whilst we have only two initial conditions on f and one initial condition on θ. The two initial condition

$f''(0)$ and $\theta'(0)$ which are not prescribed, however the values of $f'(\eta)$ and $\theta(\eta)$ are known at $\eta = \infty$. Now, we employ numerical Keller-Box scheme where these two boundary conditions are utilized to produce two unknown initial conditions at $\eta = 0$. To select η_∞, we begin with some initial guess values for the unknown initial conditions and solve the boundary value problem to obtain $f''(0)$ and $\theta'(0)$. Let α_0 and β_0 be the correct values of $f_3(0)$ and $\theta_2(0)$, respectively and integrate the system using the fourth order Runge-Kutta method and denote the values of $f_3(0)$ and $\theta_2(0)$ respectively. The solution process is repeated with another larger value of η_∞ until two successive values of unknown conditions differ only after desired digit signifying the limit of the boundary along η. The last value of η_∞ is chosen as appropriate value for that particular set of parameters. Finally the problem has been solved numerically using a second order finite difference scheme known as Keller Box method [33-36].

The numerical solutions are obtained in four steps as follows:

- reduce equations (11) and (12) to a system of first-order equations;
- write the difference equations using central differences;
- linearize the algebraic equations by Newton's method, and write them in matrix-vector form; and
- solve the linear system by the block tri-diagonal elimination technique.

For numerical calculations, a uniform step size of $\Delta\eta = 0.01$ is found to be satisfactory and the shooting error was controlled with an error tolerance of 10^{-6} in all the cases. To assess the accuracy of the present method, comparison of the skin friction and the wall temperature gradient between the present results and previously published results are used, for several special cases.

6. RESULTS AND DISCUSSION

Employing the above numerical method, the governing equations of the problem are solved for several sets of values of the parameters. The numerical results thus obtained are presented for velocity and temperature in Figures 1-4. Also the numerical results for the Nusselt number and the skin friction are presented in Tables 1-3. The horizontal velocity profiles are presented in Figures 1(*a*)-1(c), whereas the temperature profiles are shown in Figures 2-4.

Figures 1(*a*)-1(c) respectively, show the effects of a lateral mass flux parameter [suction $(f_w < 0)$, impermeability $(f_w = 0)$ and injection $(f_w > 0)$] on the horizontal velocity component $f_\eta(\eta)$ for different values of the power-law exponent parameter m. From these figures, it can be seen that the velocity $f_\eta(\eta)$ increases from its initial value and approaches monotonically to zero as the distance η increases from the boundary. The effect of the increasing values of the power- law exponent parameter *m* is to decrease the velocity boundary layer thickness. This is due to the fact that the effect of negative values of the parameter m is to decelerate the horizontal velocity and hence reduces the momentum boundary layer thickness. From Figures 1(*a*)-1(c), it can be seen that the suction reduces the velocity boundary layer thickness whereas the injection has the opposite effect. These results are consistent with the physical situation (see Table 1).

The graphs for the temperature profiles $\theta(\eta)$ with the space variable η for different values of the parameters are presented in Figures 2-4. The general trend here is that the temperature distribution is unity at the wall and tends asymptotically to zero as the distance η increases from the boundary. Figure 2(*a*) explores the effects of the parameter m on the temperature profile $\theta(\eta)$ in the presence of lateral mass transfer parameter namely suction $(f_w = -1.0)$, with Pr = 0.72. It is observed that the effect of the parameter m is to increase the temperature $\theta(\eta)$ and hence increase the thermal boundary layer thickness. From Figures 2(*a*)-2(c), we see that the thermal boundary layer is thicker in the case of suction $(f_w = -1)$ as compared to the case of impermeability $(f_w = 0)$: However, thinner in the case of blowing $(f_w = 1)$.

The effect of the wall temperature parameter n on the temperature field $\theta(\eta)$ in the cases of suction and impermeability are depicted in Figures 3(*a*)-3(b) for different values of the parameter *m*. From these figures we see that the temperature distribution is lower throughout the boundary layer for positive values of the wall temperature

parameter n when the environment temperature is fixed or when the environment is non-stratified $(n=0)$. The effect of increasing values of the wall temperature parameter is to decrease the temperature profile and thus decrease the thermal boundary layer thickness. This is true even for different values of the power-law exponent parameter. From Figures 3(*a)*-3(b), we also observe that the environment is stably stratified if the power-law exponent parameter and the wall temperature parameter have the same sign. The variations of $\theta(\eta)$ for different values of the Prandtl number $\Pr$ and the wall temperature parameter n are displayed in Figures 4(*a*)-4(b) with changes in f_w. The effect of increasing values of the Prandtl number $\Pr$ is to decrease the temperature $\theta(\eta)$. That is, an increase in Prandtl number $\Pr$ means decrease in the thermal diffusivity α and hence it leads to a decrease of energy transfer and that decreases the thermal boundary layer thickness. This can be seen for all values of the lateral mass flux parameter.

The impact of all the physical parameters on the skin friction $[-f_{\eta\eta}(0)]$ and the wall temperature gradient $[-\theta_\eta(0)]$ can be analyzed from Tables 1-3. From Table 1 it can be seen that the effect of decreasing values of the power-law exponent parameter is to increase the skin friction as well as the wall temperature gradient. This is even true for all values of the lateral mass flux parameter. The effect of wall temperature parameter is to decrease the Nusselt number for linear shrinking (see Tables 2 and 3). The effect of the Prandtl number is to decrease the wall temperature gradient for $(n \geq -1)$ and a reverse phenomenon is true for $(n < -1)$.

REFERENCES

1. T. Altan, S. Oh, H. Gegel: Metal forming and applications. Metals park, OH: American Society of Metals (1979).
2. E. G. Fisher: Extrusion of plastics, New York: Wiley (1976).
3. Z. Tadmor, I. Klein: Engineering principles of plasticating extrusion, polymer science and engineering series, New York: Van Norstrand Reinhold (1970).
4. B.C. Sakiadis: Boundary layer behavior on continuous solid surfaces: I. Boundary-layer equations for two dimensional and axisymmetric flow, A. I. Ch. E. J. **7** (1961) 26-28.
5. B. C. Sakiadis: Boundary layer behavior on continuous solid surfaces: II, the boundary layer on a continuous flat surface, A. I. Ch. E. J. **7** (1961) 221-225.
6. L. E. Erickson, L.C. Cha, L. T. Fan: The cooling of a continuous flat sheet, AICHE Chemical Engineering Progress Symposium series, Heat Transfer-Los Angeles **62** (1966) 157-165.
7. F. K. Tsou, E. M. Sparrow, R. J. Goldstein: Flow and heat transfer in the boundary layer on a continuous moving surface, Int. J. Heat Mass Transfer **10** (1967) 219-235.
8. L. J. Crane: Flow past a stretching plate, ZAMP **21** (1970) 645-647.
9. L. J. Grubka, K. M. Bobba: Heat transfer characteristics of a continuous stretching surface with variable temperature, ASME J. of Heat Transfer **107** (1985) 248-250.
10. C.H. Chen: Laminar mixed convection adjacent to vertical continuously stretching sheets, Heat Mass Transfer **33** (1998) 471-476.
11. P. S. Gupta, A. S. Gupta: Heat and mass transfer on a stretching sheet with suction or blowing, Can. J. Chem. Engng **55** (1977) 744-746.
12. C. K. Chen, M. I. Char: Heat transfer of a continuous stretching surface with suction or blowing, J. Math. Anal. Appl. **135** (1988) 568-580.
13. M. E. Ali: Heat transfer characteristics of a continuous stretching surface, Heat Mass Transfer **29** (1994) 227-234.
14. B. Siddappa, M. S. Abel: Non-Newtonian flow past a stretching surface, *Z.* Angew Math. Phys. **36** (1985) 890 – 892.
15. R. Cortell: Viscous flow and heat transfer over a nonlinearly stretching sheet, Appl. Math. Compt. **184** (2007) 864-873.
16. B. K. Dutta, P. Roy, A. S. Gupta: Temperature field in flow over a stretching sheet with uniform heat flux, Int. Comm. Heat Mass Transfer **12** (1985) 89-94.
17. S. J. Liao: A new branch of solutions of boundary layer flows over a stretching flat plate, Int. J. Heat Mass Transfer **49** (2005) 2529-2539.
18. S. J. Liao: A new branch of solution of boundary layer flows over a permeable stretching plate, Int. J. Non-Linear Mech **42** (2007) 819-830.
19. M. Miklavcic, C.Y. Wang: viscous flow due to a shrinking sheet, Q. Appl. Math. **64** (2006) 283-290.
20. T. Fang: Boundary layer flow over a shrinking sheet with power law velocity, Int. J. Heat Mass Transfer **51** (2008) 5838-5843.
21. T. Fang, J. Zhang, S. Yao: Viscous flow over an unsteady shrinking sheet with mass transfer, Chin. Phys. Lett. **26** (2009) 014703.
22. T. Hayat, Z. Abbas, T. Javed: On the analytical solution of magnetohydrodynamic flow of a second grade fluid over a shrinking sheet, J. Appl. Mech. Trans. ASME **74** (2007) 819-830.
23. M. Sajid, T. Hayat, T. Javed: MHD rotating flow of a viscous fluid over a shrinking surface, Non-linear Dynamics **51** (2008) 259-265.

24. S. Goldstein, on backward boundary layers and flow in converging passages, J. Fluid Mech **21** (1965) 33-45.
25. R.A.W. Henkes, C. J. Hoogendoorn: Laminar natural convection boundary layer flow along a heated vertical plate in a stratified environment, Int. J. Heat Mass Transfer **32** (1989) 147-155.
26. A. K. Kulkarni, H. R. Jacobs, J. J. Hwang: Similarity solution for natural convection flow over an isothermal vertical wall immersed in thermally stratified medium, Int. J. Heat Mass Transfer **30** (1987) 691-698.
27. V.I. Semenov: Similar problems of steady state laminar free convection on a vertical plate, Heat Transfer-Sov. Res **16**, (1984) 69-85.
28. R. A. Van Gorder, K. Vajravelu and I. Pop: Hydromagnetic stagnation point flow of a viscous fluid over a stretching or shrinking sheet, Meccanica, accepted (2010).
29. R. A. Van Gorder and K. Vajravelu: A general class of coupled nonlinear differential equations arising in self-similar solutions of convective heat transfer problems, Applied Mathematics and Computation **217** (2010) 460-465.
30. R. A. Van Gorder: High-order nonlinear boundary value problems admitting multiple exact solutions with application to the fluid flow over a sheet, Applied Mathematics and Computation **216** (2010) 2177-2182.
31. R. A. Van Gorder and K. Vajravelu: Multiple solutions for hydromagnetic flow of a second grade fluid over a stretching or shrinking sheet, Quarterly of Applied Mathematics, accepted (2009).
32. T. Y. Na: Computational methods in engineering boundary value problems, Academic Press, New York, (1979).
33. T. Cebeci, P. Bradshaw: Physical and Computational Aspects of Convective Heat Transfer, Springer-Verlag, New York (1984).
34. H.B. Keller: Numerical Methods for Two-point Boundary Value Problems, Dover Publ., New York (1992).
35. H. I. Andersson, K. H. Bech, B. S. Dandapat: Magnetohydrodynamic flow of a power law fluid over a stretching sheet, Int. J. Non-Linear Mech **27** (1992) 929-936.
36. K. V. Prasad, K. Vajravelu, P. S. Datti: The effects of variable fluid properties on the hydromagnetic flow and heat transfer over a non-linearly stretching sheet, Int. J. Thermal Sciences **49** (2010) 603-610.

Table 1: Values of the skin friction and the wall temperature gradient for different values of *m* when *n* = 0 and Pr = 0.72.

m	f_w=-1.0		f_w=0.0		f_w=1.0	
	f''(0)	θ'(0)	f''(0)	θ'(0)	f''(0)	θ'(0)
-1.0	0.816586	-0.669289	0.816586	-0.669289	0.816586	-0.669289
-1.5	1.149240	-0.919032	1.034832	-0.844707	0.936204	-0.779691
-2.0	1.462780	-1.152343	1.216034	-0.990666	1.023405	-0.862813
-2.5	1.762984	-1.374922	1.374025	-1.118243	1.092029	-0.929863
-3.0	2.053773	-1.589682	1.515830	-1.232926	1.148472	-0.986130
-3.5	2.337700	-1.798672	1.645553	-1.337934	1.196261	-1.034585
-4.0	2.616455	-2.003292	1.765822	-1.435344	1.237567	-1.071086
-4.5	2.891198	-2.204515	1.878436	-1.526588	1.273829	-1.114882
-5.0	3.162755	-2.403029	1.984690	-1.612699	1.306053	-1.148877

Table 2: Values of the wall temperature gradient for different values of *n* when *m* = -1.0.

n	Pr = 0.72	Pr = 1.0	Pr = 5.0
-2.0	0.612231	0.777850	2.040186
-1.5	0.291684	0.379206	1.0919861
-1.0	-0.028863	-0.019439	-0.000464
-0.5	-0.349409	-0.418082	-1.020786
0.0	-0.669289	-0.816725	-2.04111
0.5	-0.990500	-1.215370	-3.061436
1.0	-1.311046	-1.614013	-4.081760
1.5	-1.631593	-2.012659	-5.102085
2.0	-1.952139	-2.411303	-6.122409

Table 3: Values of the wall temperature gradient for different values of the physical parameters.

m	n	f_w = -1.0			f_w = 0.0			f_w = 1.0		
		Pr = 0.72	Pr = 1.0	Pr = 5.0	Pr = 0.72	Pr = 1.0	Pr = 5.0	Pr = 0.72	Pr = 1.0	Pr = 5.0
-1.5	-2.0	0.640998	0.854176	2.950970	0.731892	0.933629	2.564400	0.740231	0.910006	2.053787
	-1.5	0.250824	0.353299	1.385238	0.337741	0.441514	1.272254	0.360250	0.448454	1.026705
	-1.0	-0.139350	-0.147577	-0.180495	-0.056408	-0.050601	-0.019894	-0.019731	-0.013099	-0.000378
	-0.5	-0.529524	-0.648454	-1.746223	-0.450558	-0.542717	-1.312038	-0.399711	-0.474652	-1.027459

	0.0	-0.919697	-1.149330	-3.311956	-0.844707	-1.034831	-2.604185	-0.779691	-0.936204	-2.054542
	0.5	-1.309871	-1.650207	-4.877687	-1.238856	-1.526946	-3.896332	-1.159671	-1.397757	-3.081624
	1.0	-1.700045	-2.151083	-6.443422	-1.633006	-2.019062	-5.188478	-1.539652	-1.859310	-4.108706
	1.5	-2.09219	-2.651960	-8.009154	-2.027155	-2.511177	-6.480628	-1.919632	-2.320862	-5.135788
	2.0	-2.480393	-3.152837	-9.574886	-2.421306	-3.003292	-7.772775	-2.299613	-2.782416	-6.162871
	-2.0	0.545626	0.748536	3.129663	0.797044	1.023700	2.943483	0.829383	1.002078	2.0499726
	-1.5	0.121074	0.195704	1.196668	0.350117	0.463766	1.440418	0.406334	0.495706	1.024775
	-1.0	-0.303477	-0.357130	-0.736323	-0.096811	-0.096167	-0.062648	-0.016716	-0.010664	-0.000176
	-0.5	-0.728027	-0.909961	-2.669315	-0.543739	-0.656101	-1.565713	-0.439764	-0.517034	-1.025126
-2.0	0.0	-1.152578	-1.462794	-4.602310	-0.990666	-1.216034	-3.068779	-0.862814	-1.023404	-2.050077
	0.5	-1.577129	-2.015626	-6.535303	-1.437594	-1.775967	-4.571844	-1.285861	-1.529775	-3.075028
	1.0	-2.001681	-2.568458	-8.468296	-1.884521	-2.335901	-6.074910	-1.708910	-2.036146	-4.099979
	1.5	-2.426263	-3.121291	-10.40128	-2.331499	-2.895835	-7.577975	-2.131960	-2.542517	-5.124930
	2.0	-2.85078	-3.67412	-12.3343	-2.77838	-3.45577	-9.08104	-2.55501	-3.04889	-6.14989

Nomenclature

C constant defined in equation (2.16)
M, N coefficients in defined in equation (2.6)
f similarity stream function
f' the first derivative of f with respect to η
f'' the second derivative of f with respect to η
f''' the third derivative of f with respect to η
f_w mass transfer parameter at the sheet
g the transformed function
m power law exponent parameter
n wall temperature parameter
Nu Nusselt number
P pressure
Pr Prandtl number
q_w heat flux from the surface
Re_ξ the local Reynolds number
T temperature
T_c constant defined in equation (2.6)
T_w temperature of the plate
T_∞ ambient temperature
ΔT characteristic temperature difference
u fluid velocity in *x*-direction
v fluid velocity in *y*-direction
x coordinate along the shrinking sheet
y coordinate perpendicular to the *x*-direction
U_w a constant

Greek symbols

α effective thermal diffusivity of the fluid
α_0, β_0 initial guess value
η similarity variable
ξ transformed *x*-co ordinate $Mx + N$
$\Delta\eta$ grid size in the η direction
θ nondimensional temperature
θ' the first derivative of θ with respect to η
$\wp$ Weierstrass's elliptic function
κ implicit relation
μ viscosity
ν kinematic viscosity
ρ density
ψ stream function
τ_w shear stress at the surface

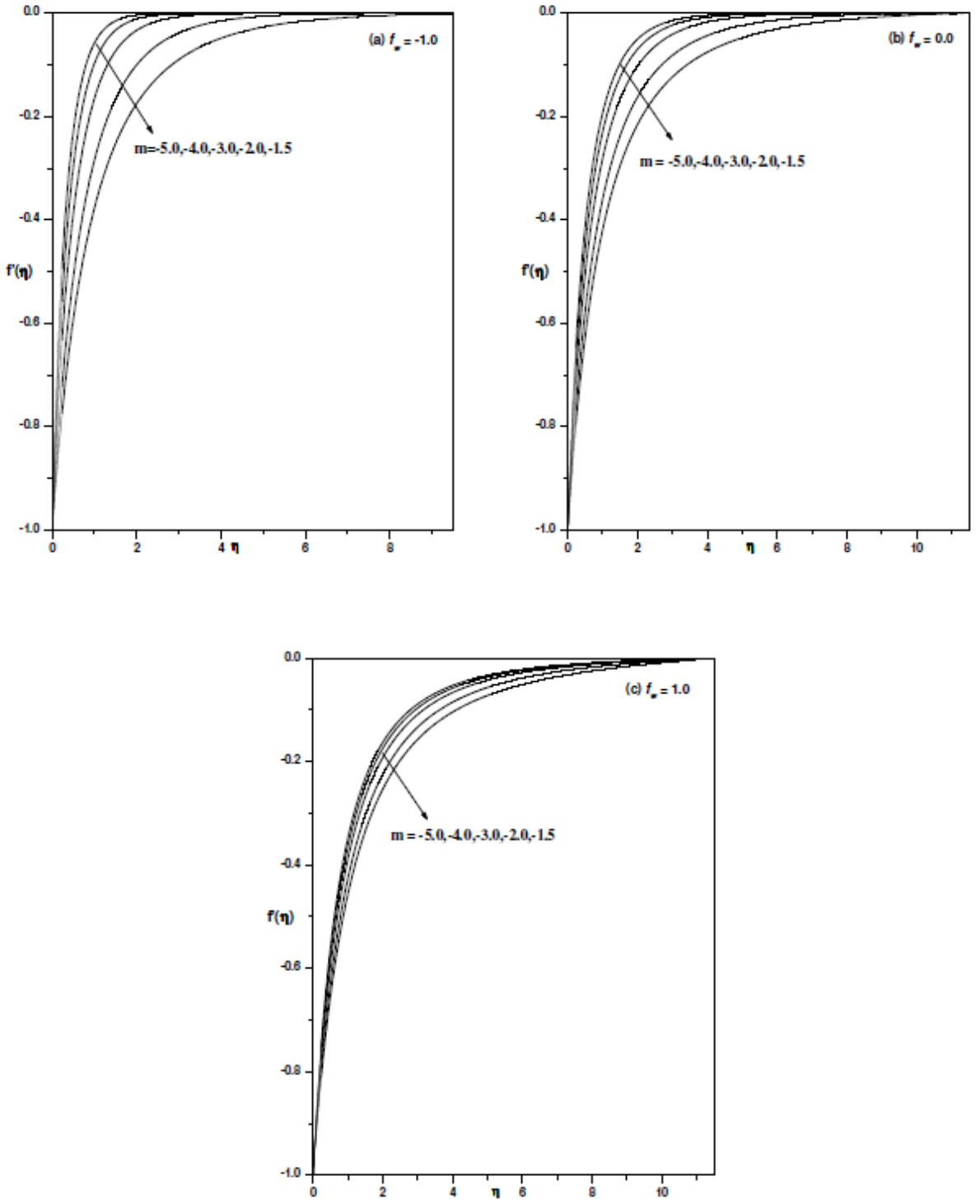

Fig.1: Horizontal velocity profiles for different values of *m* with (a) f_w = -1.0, (b) f_w = 0.0 and (c) f_w = 1.0.

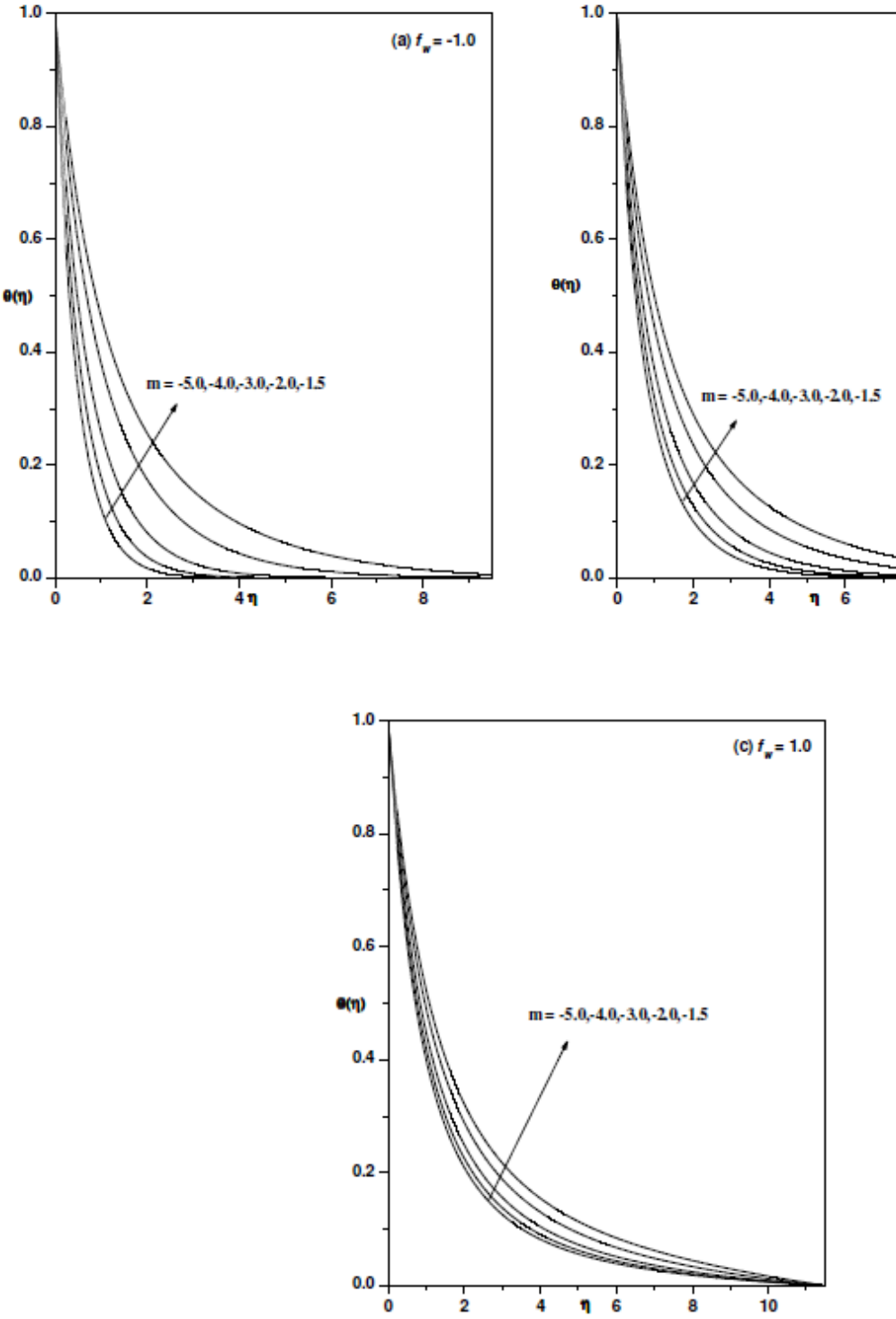

Fig.2: Temperature profiles for different values of m with Pr = 0.72 when (a) f_w = -1.0, (b) f_w = 0.0 and (c) f_w = 1.0

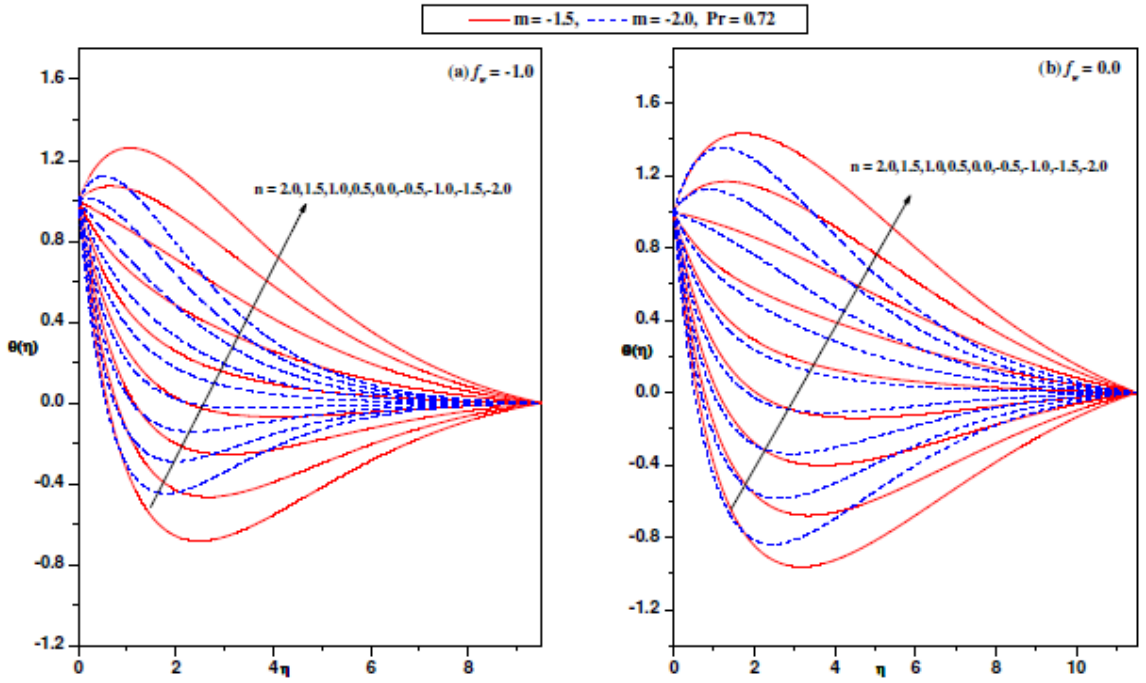

Fig.3: Temerature profiles for different values of n and m with $Pr = 0.72$ when (a) $f_w = -1.0$, and (b) $f_w = 0.0$.

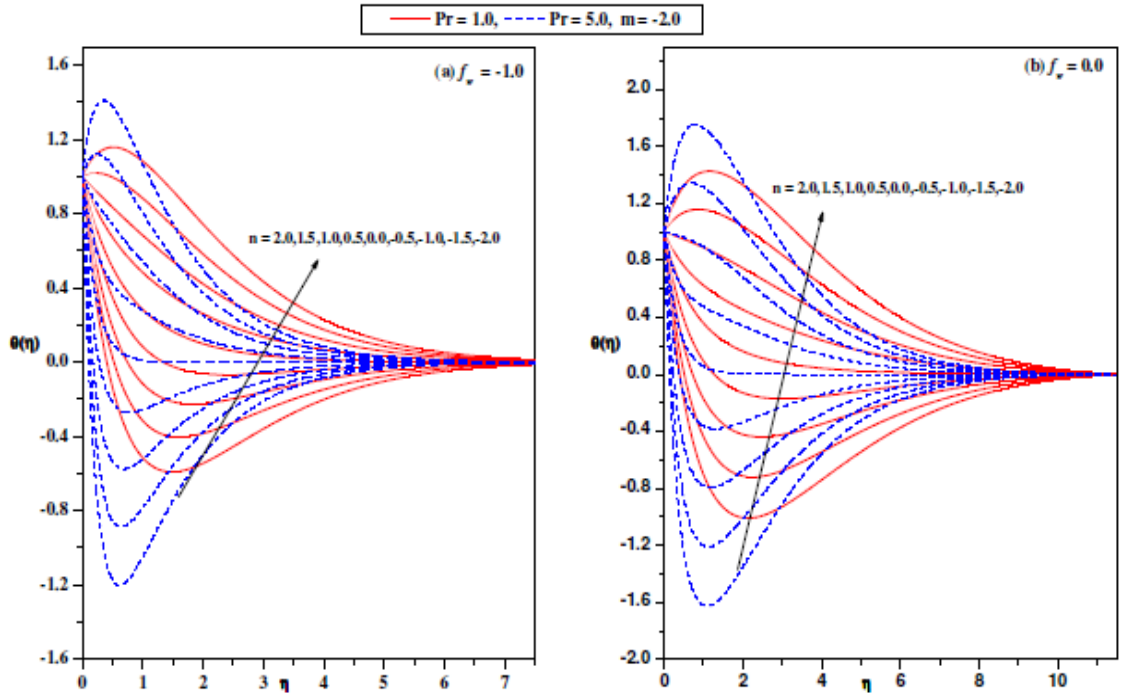

Fig.4: Temerature profiles for different values of n and Pr with $m = -2.0$ when (a) $f_w = -1.0$, and (b) $f_w = 0.0$.

Source of support: Nil, Conflict of interest: None Declared

